Regulation of Intracellular Cl^- Levels by Na^+-Dependent Cl^- Cotransport Distinguishes Depolarizing from Hyperpolarizing $GABA_A$ Receptor-Mediated Responses in Spinal Neurons

Jeffrey Rohrbough and Nicholas C. Spitzer

Department of Biology and Center for Molecular Genetics, University of California at San Diego, La Jolla, California 92093-0357

Rohon–Beard (RB) spinal neurons of *Xenopus* larvae are depolarized by GABA. To study the mechanisms underlying this distinctive response, intracellular and patch-clamp recordings were made from RB neurons *in situ*. The intracellularly recorded GABA reversal potential (E_{Rev}) was near −30 mV in normal saline and was ~25 mV more negative in Na^+-free saline. Whole-cell recordings from RB neurons and from neighboring dorsolateral interneurons (DLi) revealed that GABA responses of both cells were mediated by $GABA_A$ receptors. Currents elicited by GABA were mimicked by muscimol and reversibly blocked by bicuculline, and E_{Rev} shifted with changes in Cl^- concentration ($[Cl^-]$) in agreement with Cl^- selectivity. In perforated patch recordings, E_{Rev} for RB cells was significantly more positive than for DLi cells (−38 vs −63 mV), indicating that intact RB cells maintain higher levels of intracellular Cl^-. Replacement of external Na^+ or exposure to the Cl^- transport inhibitor bumetanide (100 μM) shifted RB cell E_{Rev} to more negative values, consistent with Na^+-dependent Cl^- cotransport contributing to higher internal $[Cl^-]$. In contrast, these treatments did not change DLi cell E_{Rev}. The results indicate that a Na^+-dependent Cl^- transport mechanism underlies $GABA_A$ receptor-mediated depolarizing Cl^- conductances in RB neurons. Thus, both inhibitory and excitatory GABA responses appear to be present during the same developmental period *in vivo*. GABA may stimulate Ca^{2+} influx in RB neurons because the intracellular GABA E_{Rev} is above the threshold for low voltage-activated Ca^{2+} channels.

Key words: GABA; depolarization; chloride; chloride transport; spinal neurons; development

GABA is the major inhibitory transmitter in the adult mammalian CNS, exerting a hyperpolarizing influence primarily through the activation of $GABA_A$ receptor Cl^- channels (Cherubini et al., 1991; MacDonald and Olsen, 1994). In contrast, GABA acting at $GABA_A$ receptors depolarizes and excites immature neurons in the mammalian hippocampus (Mueller et al., 1984; Janigro and Schwartzkroin, 1988b; Ben-Ari et al., 1989; Cherubini et al., 1990), where GABA-mediated excitation may be important before the development of glutamatergic innervation (Cherubini et al., 1991). Similarly, GABA and glycine mediate depolarizing responses in developing mammalian motoneurons (Wu et al., 1992) and dorsal horn neurons (Reichling et al., 1994; Wang et al., 1994). These findings suggest that many immature neurons have elevated levels of intracellular Cl^- ($[Cl^-]_i$). In the hippocampus, hyperpolarizing $GABA_A$ responses appear during the second postnatal week, consistent with a developmental increase in the Cl^- gradient resulting from the appearance of outwardly directed Cl^- transport during this period (Zhang et al., 1991). Reciprocally, inwardly directed Cl^- transport, as has been reported in adult guinea pig hippocampal neurons (Misgeld et al., 1986), could be a mechanism underlying the reduced Cl^- gradient in immature cells. Presently, however, there appears to be no evidence for such a mechanism in young neurons.

Primary sensory Rohon–Beard (RB) neurons in the developing *Xenopus* spinal cord are depolarized by GABA (Bixby and Spitzer, 1982). In intracellular recordings, the GABA reversal potential was near −30 mV and shifted toward more negative values in Na^+-free external saline, suggesting a GABA-activated cationic conductance. Because spontaneous elevations of intracellular Ca^{2+} levels ($[Ca^{2+}]_i$) are involved in regulating differentiation of *Xenopus* spinal neurons (Gu and Spitzer, 1995), an increased understanding of the depolarizing action of GABA and glycine on sensory neurons is of considerable interest.

We determined the ionic basis of the depolarizing GABA response in RB neurons of *Xenopus* larvae and compared the responses with those of neighboring dorsolateral interneurons (DLi), which receive inhibitory GABAergic and glycinergic synaptic input (Clarke and Roberts, 1984; Sillar and Roberts, 1991; Sillar and Simmers, 1994). Whole-cell recordings show that both the depolarizing response in RB cells and the inhibitory response in DLi cells are mediated by $GABA_A$ receptors. To address the mechanism of the differences between these cells in their normal intact condition, we carried out amphotericin B- and gramicidin-perforated patch recordings (Horn and Marty, 1988; Rae et al., 1991; Kyrozis and Reichling, 1995) to minimize alteration of $[Cl^-]_i$. Under these conditions, the GABA reversal potential of RB cells is ~25 mV more positive than for DLi cells, presumably because of a higher $[Cl^-]_i$ (Rohrbough and Spitzer, 1994). We show for the first time that a Na^+-dependent inward Cl^- transport mechanism contributes to this elevated $[Cl^-]_i$ in developing spinal neurons. GABA, therefore, may generate depolarizations suffi-

Received July 13, 1995; revised Sept. 13, 1995; accepted Sept. 19, 1995.

This work was supported by National Institutes of Health Grants T32 NS07220 and NS09603 (J.R.) and NS15918 (N.C.S.). We thank Drs. E. Gleason, Z.-w. Zhang, and S. Meriney for their helpful comments on the manuscript and S. Watt and I. Hsieh for expert technical assistance.

Correspondence should be addressed to Nicholas C. Spitzer, Department of Biology, 0357, University of California at San Diego, 9500 Gilman Drive, La Jolla, CA 92093-0357.

Table 1. Composition of recording solutions (in mM)

A. Intracellular recordings		NaCl	TrisCl or TEACl	KCl	$CaCl_2$	HEPES	Base			
	B1 (Normal)	125	0	3	10	5	2 NaOH			
	B2 (Na^+-free)	0	120	3	10	5	17 Tris base			
B. Whole-cell recordings		**NaCl**	**NaIsethionate**	**KCl**	**$CaCl_2$**	**$CdCl_2$**	**$CoCl_2$**	**HEPES/NaOH**		
External	B3 (132.4Cl^-)	125	0	3	2	0.2	0	5		
	B4 (106.4 Cl^-)	99	26	3	2	0.2	0	5		
	B5 (168 Cl^-)	125	0	3	10	0	10	5		
	B6 (43 Cl^-)	0	125	3	10	0	10	5		
	B7 (43.4 Cl^-)	36	89	3	2	0.2	0	5		
		KGluconate	NaGluconate	$CsMeSO_3$	CsCl	NaCl	$CaCl_2$	EGTA	HEPES	Base
Pipette	P1 (16.4 Cl^-)	85	0	0	0	10	3.2	5	10	22 KOH
	P2 (16.4 Cl^-)	0	0	90	0	10	3.2	5	10	23 CsOH
	P3 (106.4 Cl^-)	0	0	0	90	10	3.2	5	10	21 CsOH
	P4 (6.4 Cl^-)	0	10	90	0	0	3.2	5	10	21 CsOH
C. Perforated patch recordings		**NaCl**	**NaIsethionate**	**TrisCl**	**KCl**	**$CaCl_2$**	**$CdCl_2$**	**TEACl**	**HEPES**	**Base**
External	B8 (+Na^+)	125	0	0	3	2	0.2	20	5	2 NaOH
	B9 (Na^+-free)	0	0	125	3	2	0.2	20	5	15 Tris base
	B10 (Na^+/K^+-free)	0	0	128	0	2	0.2	20	5	15 Tris base
	B11 (31.4 Cl^-)	0	125	0	3	2	0.2	20	5	2 NaOH
		KGluconate	NaGluconate	NaCl	$CaCl_2$	KOH	HEPES			
Pipette	PP1	100	0	10	5	5	10			
	PP2	100	5	5	5	5	10			

All external solutions contained 0.25 μg/ml TTX. $MgCl_2$ (2–10 mM) was included in external salines in some experiments to retard muscle activity. For reversal potential determinations in intracellular recordings, $CoCl_2$ (10 mM) and TEACl (20 mM) were included in solutions B1 and B2. In initial whole-cell recordings, external solutions contained 10 mM $CaCl_2$ and $CoCl_2$ (B5 and B6) for consistency with intracellular recording solutions. In most whole-cell experiments, solutions B3, B4, and B7 were used. Solutions P1–P4 contained 2 mM Mg-ATP.

cient to activate low voltage-activated Ca^{2+} channels and to elevate $[Ca^{2+}]_i$ in RB cells. The contrasting actions of GABA in these two types of larval spinal neurons demonstrate that, as in the hippocampus, GABA may serve both excitatory and inhibitory roles in the developing amphibian spinal cord.

MATERIALS AND METHODS

Preparation. Experiments were performed on 3- to 8-d-old *Xenopus laevis* larvae (stages 36–48; Nieuwkoop and Faber, 1965). Preparations were dissected and mounted for recording by methods similar to those of Baccaglini and Spitzer (1977). Animals were pinned into Sylgard-coated 35 mm culture dishes in standard amphibian Ringer's solution [(in mM) 125 NaCl, 3 KCl, 10 $CaCl_2$, 10 HEPES, pH 7.4] or recording solution (Table 1) and decapitated. Trunk skin and dorsal tail muscle were removed with jeweler's forceps and an electrolytically sharpened tungsten needle. A thin, nearly transparent sheath consisting of meningeal membrane and fiber tracts remained overlying the dorsal aspect of the spinal cord. Because of their superficial position, RB neurons could be impaled with microelectrodes through this sheath. However, to make GΩ seals successfully from dorsal neurons in patch-clamp experiments, this surface had to be scored carefully with the tungsten needle to expose cell bodies. RB neurons were identified by their size (20–25 μm diameter) and position in the dorsal midline. Usually, recordings could be attempted from only a few of the ~200 RB cells per preparation. Dorsolateral neurons are positioned in the dorsal quarter of the cord just lateral to RB cells and have cell body diameters of 10–15 μm. Nearly all of these cells are likely to be either dorsolateral commissural or ascending interneurons (Roberts and Clarke, 1982; Clarke and Roberts, 1984; Sillar and Simmers, 1994). By the convention established by Sillar and Simmers (1994), they are denoted here as DLi. The preparation was visualized at 500× with Zeiss interference contrast optics.

Electrophysiological recordings. Preparations were superfused constantly with recording saline (~2 ml/min). A bath volume of ~0.5 ml was maintained, and an agar bridge between the Ag–AgCl reference electrode and the bath solution was used in all experiments. For conventional intracellular recordings, voltages and injected currents were measured with a WP Instruments amplifier (model M4-A). RB cells were impaled, usually by brief capacitance overcompensation, with glass microelectrodes filled with 3 M KCl (80–120 MΩ resistances). Data were accepted for cells with resting potentials >-40 mV. Injection of current for which the electrode remained in balance ($<\pm 0.3$ nA) was used to adjust the membrane potential to different steady levels and to assess membrane conductance with current pulses. Voltage responses to bath-applied 100 μM GABA or to brief (<50 msec) focal iontophoretic pulses from high-resistance microelectrodes containing 3–4 M GABA were recorded at membrane potentials negative to −40 mV. In previous intracellular recordings of GABA responses from RB neurons *in vivo*, similar results were obtained with either KCl-filled or K^+-acetate-filled microelectrodes (Bixby and Spitzer, 1982); therefore, we did not consider leakage of Cl^- from the electrodes to alter significantly the estimated GABA reversal potential. Signals were displayed on an oscilloscope, and permanent records were made to a Gould Brush pen recorder.

Whole-cell and perforated patch voltage-clamp recordings were made with a Dagan 8900 amplifier. The TL-1 interface hardware and pClamp software (Axon Instruments, Foster City, CA) were used for data acquisition and analysis. Patch pipettes were pulled from 100 μl capillaries (Drummond, Broomall, PA) with a Flaming/Brown electrode puller (model P-87, Sutter Instruments, Novato, CA) and had 3–5 MΩ resistances when filled with pipette solutions (Table 1). Seals were formed on exposed and clearly visualized somata of cells by applying gentle suction to the pipette. Stable patch-clamp recordings from cells *in vivo* were more difficult to achieve than from cultured embryonic spinal neurons. In general, however, the success rate of both recording modes was several-

fold higher for DLi cells than for RB cells. Series resistance (R_S) was estimated from the extrapolated peak current of transients (digitized at 50 kHz) generated by a 10–15 mV depolarizing step from −80 mV. In most cases the transient decay could be fit with a single exponential time constant. In some cases the fit was improved with a second exponential with a slower time constant and a minor fractional area (10 ± 10% of the area of the primary component). Adequate voltage-clamp control over the soma was assumed for cells in these categories, and all reversal potentials were determined from responses to focal application of agonist to somata. R_S typically was 4–10 MΩ in whole-cell recordings. Voltage corrections for R_S were applied to the data and did not exceed a few millivolts because the recorded currents were usually several hundred picoamperes or less.

Perforated patch recordings were made using amphotericin B or gramicidin. Amphotericin B is similar to nystatin in its selectivity for monovalent cations over Cl^-, whereas multivalent ions are impermeant. The permeability to Cl^- is 0.03–0.1 relative to the permeability to Na^+ and K^+ in 10–100 mM salt solutions (Cass et al., 1970; Marty and Finkelstein, 1975; Russell et al., 1977; Kleinberg and Finkelstein, 1984). A K^+ gluconate pipette solution containing 15 or 20 mM Cl^- (Table 1) was used for amphotericin B-perforated patch recordings from both classes of cells to reduce possible changes in $[Cl^-]_i$ over time because of equilibration with the pipette solution. We also made recordings from DLi cells using gramicidin, which is impermeant to Cl^- (Hladky and Haydon, 1984; Rhee et al., 1994; Kyrozis and Reichling, 1995) to verify that shifts in $[Cl^-]_i$ using amphotericin B were minor or negligible. Stocks of amphotericin B or gramicidin in dimethyl sulfoxide (DMSO; 60 mg/ml, Fisher Scientific, Pittsburgh, PA) were prepared daily and frozen. One milliliter of filtered pipette solution was added to an aliquot of freshly thawed stock plus 8 μl of 20% pluronic (Molecular Probes, Eugene, OR) for final antibiotic concentrations of 120–240 μg/ml (amphotericin B) and 30–50 μg/ml (gramicidin). This mixture was vortexed for ~30 sec, sonicated for ~15 sec, and (for amphotericin B) stored on ice in the dark during experiments. Fresh 1 ml mixtures were made every 1–2 hr. Pipettes were dipped for ~5 sec in standard pipette solution to fill the tip and then back-filled with the antibiotic solution. A slight positive pressure was applied to the pipette until a cell was contacted. Access resistance after seal formation was estimated from current transients recorded at frequent intervals. In our preparation, R_S typically decreased to 20–50 MΩ, but little thereafter. Recordings were begun as soon as R_S reached this range, within several minutes in many cases when using amphotericin and generally within 8–10 min when using gramicidin. Gramicidin-perforated patch recordings from RB cells were unsuccessful because of invariable deterioration and eventual loss of the seal during this period. Partial R_S compensation (~50%) was applied during data acquisition. Additional voltage correction, typically no more than several millivolts, was applied during data analysis to achieve complete compensation.

Reversal potential determination. In intracellular recordings, the GABA reversal potential (E_{Rev}) was determined from voltage responses to iontophoretically applied GABA by linear extrapolation of response amplitudes plotted against membrane voltage. In most whole-cell and perforated patch experiments, GABA was applied with brief iontophoretic pulses (20–50 msec). In some experiments, 100 μM GABA dissolved in external saline was applied by a pressure pipette (100–200 msec, 5–10 psi). These two modes of focal GABA application elicited comparable currents, and there was no difference between the average E_{Rev} values recorded with the two methods under the same ionic conditions. Muscimol (100–150 μM) was applied by pressure pipette. GABA E_{Rev} values were determined by recording over a range of voltages in which agonist currents reversed in polarity. The agonist current was determined from the peak response amplitude after subtraction of the baseline just before the response.

In initial perforated patch recordings, we observed that E_{Rev} of the smaller DLi cells could be shifted transiently in the positive direction by strong outward currents elicited by GABA at depolarized voltages or by repeated or lengthy (>10 sec) depolarizing steps. Accordingly, GABA responses were elicited during a 1–2 sec voltage step from a holding potential of −60 or −70 mV, and depolarizing steps were applied that were just sufficient to reverse the current. Intracellular Cl^- activity ($a[Cl^-]_i$) was estimated from the reversal potential and external aCl^- using the Nernst equation. Estimates of the total aCl^- for all solutions were made from the sum of activities for individual Cl^- salts (Robinson and Stokes, 1965). Current traces were low-pass-filtered at 1–5 kHz and digitized to disk at 0.5–1 kHz. Selected records were refiltered digitally at 200–1000 Hz for display. All values in the text and figures are presented as mean ± SD; significance was assessed by Student's two-tailed t test, and values are indicated to be significantly different for $p < 0.05$.

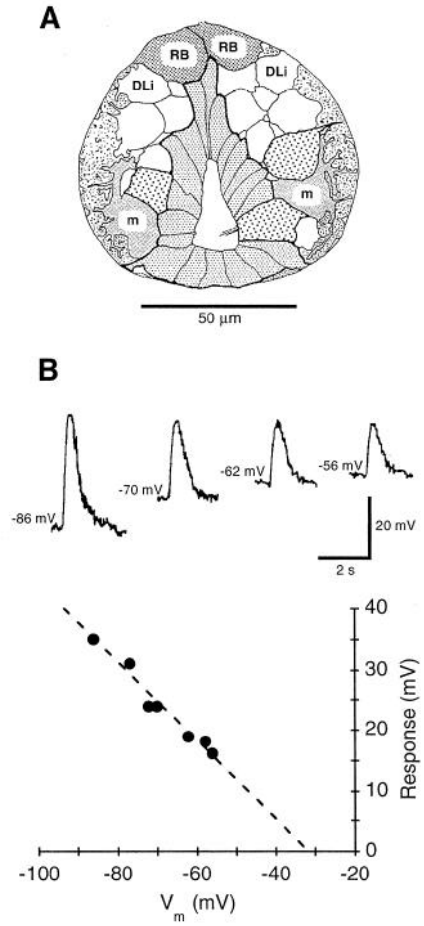

Figure 1. Depolarizing responses of RB neurons to iontophoretic application of GABA. *A*, Schematic anatomical representation of neurons in a transverse section of the *Xenopus* larval spinal cord. *RB*, Rohon–Beard cells; *DLi*, dorsolateral interneurons; *m*, motoneurons; after Roberts and Clarke (1982), with permission. *B*, Depolarizations recorded intracellularly in response to focal iontophoretic applications (50 msec) of GABA in normal saline (*top*), and plot of response amplitude versus membrane potential (*bottom*). Solution B1; 3.5-d-old larva. Membrane voltage is indicated for each trace. The extrapolated reversal potential determined by least-squares regression (*dotted line*) is −32 mV.

Solutions. The compositions of external and pipette solutions are listed in Table 1. Additionally, whole-cell pipette solutions contained 2 mM Mg-ATP, and all external solutions contained 0.25 μg/ml TTX. NaCl, KCl, $MgCl_2$, and $CaCl_2$ were obtained from Fisher Scientific (Tustin, CA), HEPES was obtained from Research Organics (Cleveland, OH), and all other chemicals and drugs were obtained from Sigma (St. Louis, MO). Liquid junction potentials between bath and pipette solutions were measured (Neher, 1992) for each combination used in whole-cell and perforated patch experiments. Corrections for liquid junction potentials were applied to the data and varied from −3 mV (solutions B4 and P3) to −18 mV (solutions B10 and PP1).

RESULTS

Depolarizing GABA responses in intracellular recordings from RB cells

GABA applied by bath perfusion (100 μM) or by iontophoresis generated depolarizations in RB cells of up to 40 mV in intracellular recordings (Fig. 1*A,B*). GABA depolarizations were accompanied by two- to fivefold increases in membrane conductance from resting values (3.6 ± 0.9-fold, $n = 12$). E_{Rev} was estimated

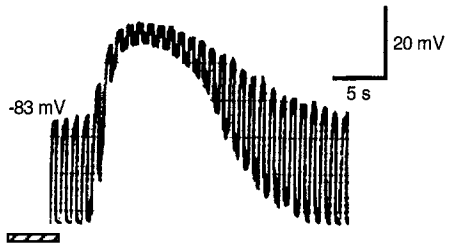

Figure 2. Depolarization and membrane conductance increase in response to bath application of GABA in whole-cell recording. Current clamp recording from a 7-d-old larva. GABA (100 μM) was applied in the bath for 5 sec (*hatched bar*). The increase in membrane conductance is indicated by the size of the voltage excursions to 0.02 nA hyperpolarizing current pulses (not shown). The delay in response onset is a result of the lag in the perfusion system. Solutions B1 and P1.

from voltage responses elicited at different membrane potentials to iontophoretically applied GABA (Fig. 1*B*). To minimize the activation of voltage-gated conductances by depolarization, blocking agents (TTX, TEA, and Co^{2+}; Table 1) were included in the external saline, and responses were recorded at membrane potentials negative to −40 mV. E_{Rev} was −29 ± 4 mV in normal saline (n = 9), which is in good agreement with the intracellular E_{Rev} reported previously under the same ionic conditions (Bixby and Spitzer, 1982). These authors found E_{Rev} to be 35 mV more negative in Na^+-free external saline, an unexpected result for a response mediated by $GABA_A$ receptors. As a first step in examining the ionic basis of the depolarizing response, we recorded responses in Na^+-free external saline to confirm this effect. When Na^+ was replaced with Tris or TEA, the extrapolated E_{Rev} was −55 ± 6 mV (n = 16). This 25 mV negative shift in E_{Rev} confirmed the involvement of Na^+ in the GABA response of RB neurons; however, the magnitude of the shift was substantially less than that expected for a Na^+-selective conductance.

GABA responses in RB cells are mediated by Cl^- conductance in whole-cell recordings

In initial whole-cell recordings, responses were recorded in current clamp mode to bath-applied GABA in normal and Na^+-free saline to address the Na^+ dependence of the GABA response. Application of 100 μM GABA produced depolarizations that reversed in polarity near −50 mV (solutions B1 and P1) and large increases in membrane conductance (5.7 ± 2.7-fold increase, n = 20; Fig. 2). Replacing external Na^+ with Tris did not alter the response amplitude or conductance increase or shift the whole-cell GABA E_{Rev} (n = 9), which is inconsistent with the contribution of a Na^+ conductance to the GABA response.

We therefore examined the Cl^- dependence of the RB cell GABA response in whole-cell voltage-clamp recordings (Fig. 3). GABA applied focally by iontophoresis or by pressure pipette (100 μM) elicited inward currents that reversed at −50 ± 2 mV (n = 5; solutions B5 and P2). Reducing external $[Cl^-]$ to 43 mM resulted in a positive shift in E_{Rev} to −22 ± 2 mV (n = 5), indicating dependence on Cl^-. For four additional combinations of external and pipette $[Cl^-]$, the whole-cell E_{Rev} varied in a manner consistent with selectivity for Cl^-, characteristic of a $GABA_A$-type response (Fig. 3*C*). The E_{Rev} shifted with a slope of 54 mV per 10-fold change in the ratio of external to pipette $a[Cl^-]$, a value reasonably close to that predicted from the Nernst equation assuming Cl^- selectivity.

RB cell GABA responses exhibit $GABA_A$ receptor pharmacology

GABA responses were reversibly blocked by the competitive $GABA_A$ receptor antagonist bicuculline methiodide (BMI; Fig. 4). BMI (50–100 μM) applied to the superfusate for 1–2 min reversibly blocked ~80% of the peak current evoked by iontophoretically applied GABA (n = 5). The incomplete blockade under these conditions was probably caused by application of GABA at concentrations sufficient to overcome competitive inhibition by BMI. The currents remaining in the presence of 50–100 μM BMI reversed at the same potential as control currents (Fig. 4*B*; n = 3), consistent with an incompletely blocked $GABA_A$ response. The $GABA_A$ agonist muscimol (150 μM) elicited responses in RB cells similar to those elicited by GABA (n = 5). The muscimol E_{Rev} of −46 ± 4 mV (solutions B5 and P1) did not differ significantly from that observed for GABA at the same $a[Cl^-]$ ratio. The Cl^- selectivity and characteristic $GABA_A$ pharmacology lead us to conclude that the GABA response of RB cells is mediated by $GABA_A$ receptors.

Whole-cell $GABA_A$ currents in DLi cells

DLi cells are located in the dorsal spinal cord, immediately lateral to RB cells (Fig. 1*A*) and are most likely composed of dorsal ascending and dorsolateral commissural interneurons (Roberts and Clarke, 1982; Clarke and Roberts, 1984; Sillar and Simmers, 1994). Spontaneous IPSPs mediated by GABA and glycine, as well as glutamatergic EPSPs, have been demonstrated previously in intracellular recordings from DLi cells in the spinal cord (Sillar and Roberts, 1991; Sillar and Simmers, 1994). Because the hyperpolarizing IPSPs suggest that GABA mediates an inhibitory response in these cells typical of mature neurons, whole-cell GABA responses were recorded from DLi cells in the same preparations for comparison with RB cell responses.

DLi cells were identified by their location and smaller size and by the presence of spontaneous synaptic currents in the presence of TTX and Cd^{2+} or Co^{2+} (Fig. 5*A*). Responses in DLi cells to focal applications of GABA also were mediated by $GABA_A$ receptors. The whole-cell E_{Rev} exhibited selectivity for Cl^-, shifting 55 mV per 10-fold change in the ratio of external to pipette $a[Cl^-]$ (Fig. 5). The peak currents elicited by GABA were usually larger than those observed for RB cells. This may indicate a higher receptor density on DLi somata or the activation of additional receptors on proximal neurites. As in RB cells, GABA responses in DLi cells were reversibly blocked by 50–100 μM BMI (n = 7; Fig. 5*B*). The results from whole-cell recordings indicate, therefore, that GABA responses in both RB and DLi cells are qualitatively the same and are mediated primarily by $GABA_A$ receptors.

Perforated patch recordings reveal different chloride distributions in RB and DLi cells

Because it is presently considered unlikely that whole-cell dialysis alters the ion selectivity of the receptor channel, the results indicate that the GABA response in intact RB neurons is a Cl^--mediated depolarization. The estimated GABA E_{Rev} of −30 mV in intracellular voltage recordings suggests further that $[Cl^-]_i$ is elevated in these cells. To test this hypothesis, we made amphotericin B-perforated patch recordings (Horn and Marty, 1988; Rae et al., 1991) from RB and DLi cells to indirectly assess $[Cl^-]_i$ under conditions that more closely approximate those of intact cells. The same pipette solutions containing 15 or 20 mM $[Cl^-]$ (~13–17 mM $a[Cl]^-$) were used for both cell types, and GABA

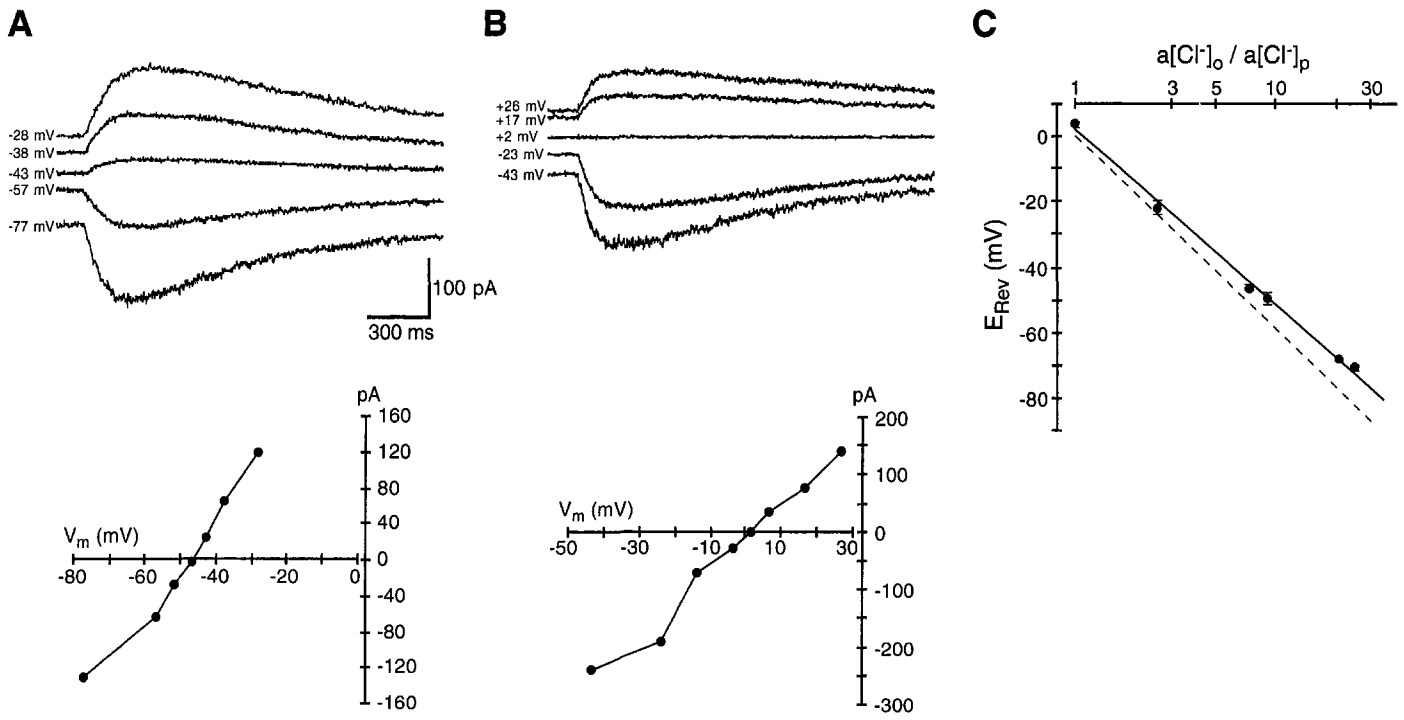

Figure 3. Chloride dependence of GABA response in RB neurons in whole-cell voltage-clamp recordings. *A*, *B*, Currents elicited by iontophoretically applied GABA (30 msec; *top*) and current–voltage (I–V) relationships (*bottom*) for two combinations of bath and pipette $[Cl^-]$. Holding potential is indicated for each current trace. Both recordings were from 8-d-old larvae. *A*, Solutions B3 (132.4 mM Cl^-) and P2 (16.4 mM Cl^-); the current reversed at −47 mV. *B*, Solutions B4 and P3 (symmetrical 106.4 mM Cl^-); the current reversed at +2 mV. *C*, Relationship of whole-cell reversal potential (E_{Rev}) to Cl^- activity ratio ($a[Cl^-]_o/a[Cl^-]_p$). Each point is the mean ± SD (where it exceeds the symbol size) for two to seven cells from 3- to 8-d-old larvae. The *dotted line* represents the predicted relationship, with a slope of −59 mV per 10-fold increase in the ratio. The *solid line* fit to the data has a slope of −54 mV per 10-fold increase.

responses were recorded in many cases within several minutes after seal formation. The E_{Rev} for RB cells was nearly 25 mV more positive than for DLi cells in standard external saline (−38 ± 3 mV, n = 22 vs −62 ± 8 mV, n = 24; Fig. 6), which is consistent with the hypothesis that $[Cl^-]_i$ is significantly higher in RB cells. This result also argues against a rapid equilibration of $[Cl^-]_i$ with the pipette solution, which would occur to a greater extent in the smaller DLi cells. Such equilibration is expected to decrease or abolish a difference in E_{Rev} between RB and DLi cells. Although there was greater variation in the E_{Rev} distribution for DLi cells, there was no consistent difference in E_{Rev} for either cell type as a function of recording times of up to 30 min, suggesting that Cl^- redistribution was not a significant source of variation under these conditions. Additionally, after several recordings, the patch was ruptured successfully and E_{Rev} was recorded in whole-cell configuration (9 DLi cells, 2 RB cells). In these cases, the whole-cell E_{Rev} always shifted in the negative direction for RB cells and in the positive direction for DLi cells, indicating that in the perforated patch configuration $[Cl^-]_i$ in these cells was significantly higher and lower, respectively, than in the recording pipette.

In perforated patch recordings, the pipette and cell contained K^+, rather than Cs^+, which was used in the internal whole-cell recording solution. We considered the possibility, therefore, that $GABA_B$ receptor activation contributes to the more negative DLi cell E_{Rev} in perforated patch recordings. Two lines of evidence suggest that this is not the case. First, when external $[Cl^-]$ was reduced to 31 mM, the DLi cell E_{Rev} shifted in the positive direction by 40 ± 7 mV (n = 3). This shift was close to the predicted change in E_{Cl} for these cells, assuming that $a[Cl^-]_i$ remained unchanged, and is consistent with a Cl^--selective $GABA_A$ conductance. Second, after patch rupture the E_{Rev} recorded in whole-cell configuration was reliably within several millivolts of E_{Cl} for the bath and pipette solutions used. Therefore, it is likely that the GABA E_{Rev} in perforated patch and intracellular recordings reflects significantly different Cl^- distributions in RB and DLi cells.

Gramicidin is a particularly attractive agent for perforated patch recordings in studies of Cl^--dependent processes because, unlike amphotericin B and nystatin, its permeability to Cl^- is negligible (Rhee et al., 1994; Kyrozis and Reichling, 1995). The gramicidin-perforated patch E_{Rev} in DLi cells was not different from that recorded using amphotericin B (−67 ± 4 mV, n = 7), further indicating that E_{Rev} was not biased significantly by redistribution of Cl^- through the perforated patch. The agreement between results obtained with either gramicidin or amphotericin B strengthens confidence in estimates of normal $a[Cl^-]_i$ in these cells and supports the reliability of results from RB cells obtained with amphotericin B. From the E_{Rev} values determined in perforated patch recordings in normal external saline (Table 2), corresponding values of $a[Cl^-]_i$ were estimated to be ~27 mM in RB cells and ~11 mM in DLi cells.

Na^+-dependent Cl^- transport contributes to the elevated $[Cl^-]_i$ in RB cells

The combination of $GABA_A$ receptor properties, elevated $[Cl^-]_i$, and Na^+ dependence of the intracellular RB E_{Rev} suggests the presence of a Na^+-dependent inward Cl^- transport mechanism. A similar mechanism for Cl^- transport has been reported in adult mammalian hippocampal (Misgeld et al., 1986) and frog dorsal

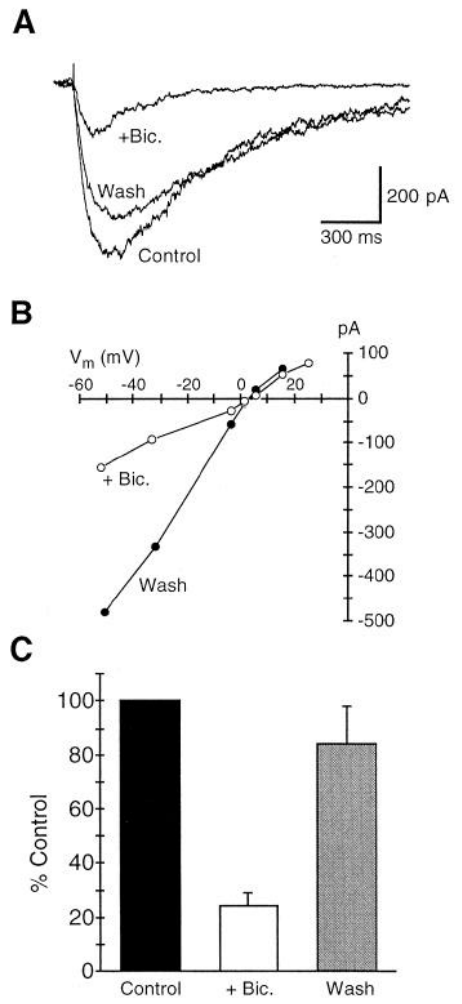

Figure 4. Bicuculline (*Bic*) blockade of GABA response in RB cells. *A*, Whole-cell currents elicited by iontophoretically applied GABA (30 msec) before, during, and after superfusion of 50 μM BMI. The holding potential is −50 mV for each trace. 4-d-old larva; solutions B4 and P3 (symmetrical $[Cl^-]$). *B*, Whole-cell I–V relationship for a different RB cell in the presence of 100 μM BMI (*open symbols*) and after washout (*solid symbols*). Solutions as in *A*. The current reversed at +3 mV in both conditions, consistent with an incompletely blocked $GABA_A$ response. 3-d-old larva. Similar results were recorded in two other RB cells. *C*, Summary of bicuculline blockade in RB cells in 3- to 8-d-old larvae (n = 5) for 50–100 μM concentrations of BMI.

root ganglion (DRG) cells (Alvarez-Leefmans et al., 1988) and has been proposed for various developing neurons. This hypothesis was tested in perforated patch recordings from RB cells. In seven cells, E_{Rev} in Na^+-free saline (substituted with Tris) shifted −9 ± 5 mV from the value recorded in standard saline. The E_{Rev} in Na^+-free saline was −48 ± 11 mV overall (n = 9; Table 2), a value significantly more negative than control (−38 ± 3 mV, n = 22). The shift after Na^+ replacement occurred within ~3 min in some cells, which represented the shortest practical interval for solution replacement and E_{Rev} measurement. This time course is consistent with the rate of change in $a[Cl^-]_i$ (4–5 mM/min) measured in frog DRG cells after removal of Na^+ (Alvarez-Leefmans et al., 1988). Furthermore, the loop diuretic bumetanide (100 μM; exposure for ≥10 min), an inhibitor of Na^+-dependent Cl^- transport (Haas, 1989), also shifted RB cell E_{Rev} by nearly 10 mV in the negative direction (−47 ± 4 mV, n = 9; Table 2). Because we were unable to maintain these recordings for extended periods of time, the full extent of the shifts caused by these treatments may not have been observed.

In contrast, DLi cells were not affected similarly by replacement of external Na^+ for comparable periods. E_{Rev} values recorded from the same cells in both normal and Na^+-free saline were not significantly different (−68 ± 4 vs −70 ± 4 mV, n = 8). Additionally, there was no effect of 100 μM bumetanide (n = 12) or a combination of 100 μM bumetanide and 300 μM ethacrynic acid (n = 5; Table 2), an inhibitor of ATP-coupled Cl^- transport (Hara et al., 1992).

Schematic model for the regulation of $[Cl^-]_i$ in RB and DLi neurons

We hypothesize a model for the regulation of $[Cl^-]_i$ in RB and DLi cells that is consistent with the difference in Cl^- distributions indicated by the GABA E_{Rev} in these cells (Fig. 7). The principal feature suggested by our results is the presence of a Na^+-dependent, bumetanide-sensitive Cl^- transport mechanism in the RB cell membrane that contributes to the elevated $[Cl^-]_i$. An additional mechanism to that proposed in the model may be involved in RB cells, because removal of external Na^+ or exposure to bumetanide in perforated patch recordings produced shifts less than half as large as the ~25 mV difference between the mean RB and DLi E_{Rev} values in standard external saline. Our results do not exclude the existence of Cl^- transporters or pumps on DLi cells; however, the absence of dependence on external Na^+ or sensitivity to bumetanide and ethacrynic acid argues against the involvement of Na^+-dependent and ATP-coupled Cl^- transport, respectively. The model thus considers DLi cells to be representative of inhibitory GABA function. Taking the GABA E_{Rev} in perforated patch recordings to be the best reflection of normal intracellular anion concentrations, $a[Cl^-]_i$ appears to differ by a factor of at least two between these cells.

DISCUSSION

Although recordings from the intact spinal cord currently present a significant technical challenge, they have potentially greater relevance than *in vitro* recordings because identified cells can be studied within a largely intact functional environment over a more extensive range of development. Our results from intracellular, whole-cell, and perforated patch recordings demonstrate that $GABA_A$ receptors mediate GABA responses in RB and DLi cells. The properties of responses of both cells are the same in whole-cell recordings. In perforated patch recordings, however, the GABA E_{Rev} of DLi cells is ~25 mV more negative than for RB cells and is not affected by removal of external Na^+ or by Cl^- transport inhibitors. The more negative reversal potential, coupled with the observation that spontaneous IPSPs recorded from DLi cells are typically hyperpolarizing (Sillar and Roberts, 1991; Sillar and Simmers, 1994), is consistent with an inhibitory function for GABA acting on DLi cells.

In contrast, GABA depolarizes RB cells because of a relatively elevated internal $[Cl^-]$. Replacement of external Na^+ or exposure to bumetanide in perforated patch recordings shifts E_{Rev} in the negative direction by ~10 mV, strongly suggesting that inwardly directed, Na^+-dependent Cl^- transport contributes to the higher $[Cl^-]_i$. These results provide evidence for a specific Cl^- transport mechanism establishing the Cl^- driving force that generates depolarizing GABA responses in the developing spinal cord. RB cells *in vivo* are sensitive to GABA from an age of 27 hr (stage 24; Bixby and Spitzer, 1982). GABA, therefore, may serve an excitatory function from an early period of development, similar to that

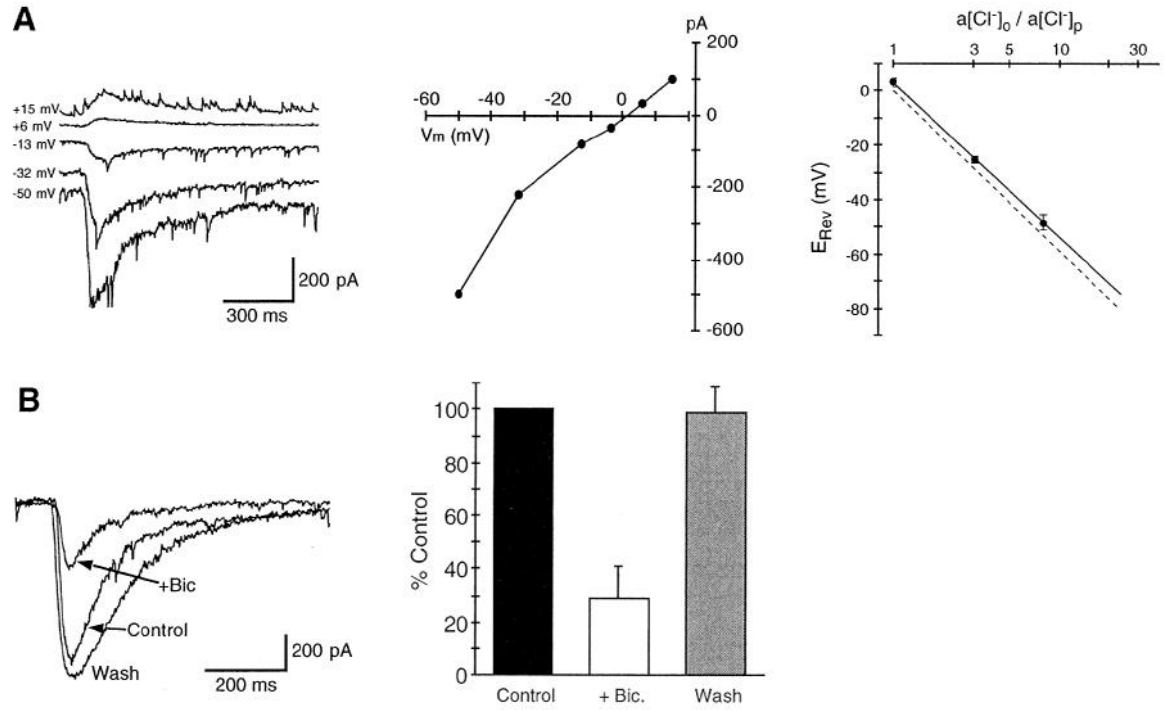

Figure 5. $GABA_A$ responses in dorsolateral interneurons. *A*, Cl^- dependence of whole-cell GABA responses in DLi cells. *Left*, Currents elicited by iontophoretically applied GABA (20 msec) at the holding potentials indicated; symmetrical $[Cl^-]$ solutions (B4 and P3). Spontaneous synaptic currents (attenuated by sampling frequency) are present. 7-d-old larva. *Middle*, I–V relationship for the same cell. The current reversed at +2 mV. *Right*, Relationship of whole-cell GABA E_{Rev} to Cl^- activity ratio ($a[Cl^-]_o/a[Cl^-]_p$). Each symbol is the mean ± SD for three to five cells from 3- to 7-d-old larvae. The *dotted line* has the predicted slope of −59 mV per 10-fold increase, as in Figure 3. The *solid line* fit to the data has a slope of −57 mV per 10-fold increase. *B*, Bicuculline (*Bic*) blockade of GABA responses in DLi cells. *Left*, GABA currents before, during, and after superfusion of 65 μM BMI for the same cell shown in *A*. The holding potential was −50 mV for each trace. *Right*, Summary of bicuculline blockade in DLi cells from 3- to 7-d-old larvae (n = 7) for 50–100 μM concentrations of BMI.

proposed for developing mammalian hippocampal and spinal neurons (Cherubini et al., 1991; Wu et al., 1992; Reichling et al., 1994). Ion transporter expression may be a developmentally regulated mechanism for altering neurotransmitter action in some neurons.

The conclusion that intact RB cells maintain higher levels of $[Cl^-]_i$ relies on the comparison of E_{Rev} values while preventing alterations in $[Cl^-]_i$. In intracellular recordings, we confirmed the finding that the RB cell GABA E_{Rev} is near −30 mV in normal saline and is 25–30 mV more negative in Na^+-free saline (Bixby and Spitzer, 1982). However, intracellular recordings had two inherent limitations, in that E_{Rev} was determined by the extrapolation of voltage responses over a limited linear range and that replacement of external Cl^- likely led to a reduction of $[Cl^-]_i$. These factors probably account for the apparent absence of dependence on external $[Cl^-]$ in the report by Bixby and Spitzer (1982), whereas the Na^+ dependence of the response suggested a cationic conductance. Perforated patch recordings of E_{GABA} pro-

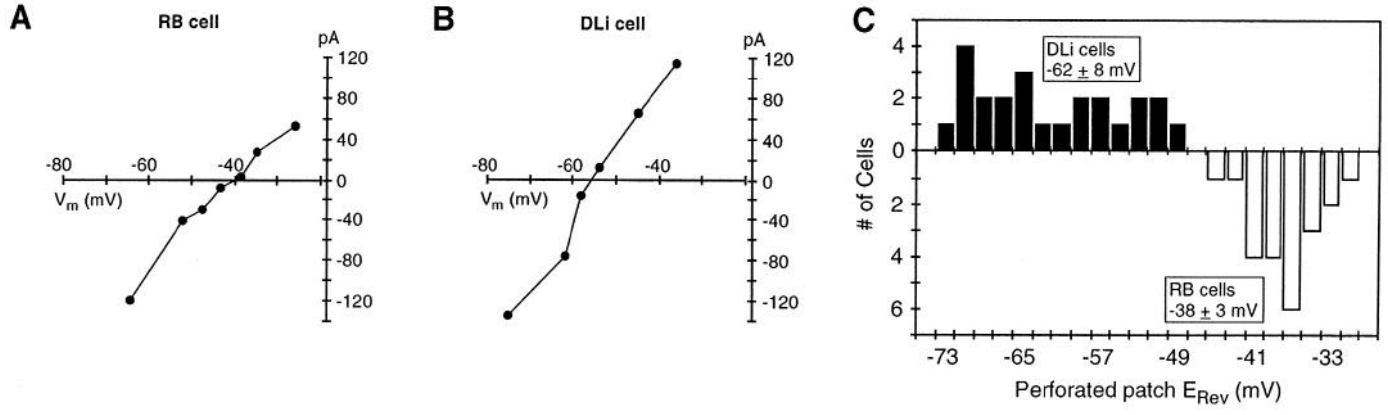

Figure 6. GABA reversal potentials in perforated patch recordings. *A* and *B*, Representative I–V relationships in perforated patch recordings in normal external saline (solutions B8 and PP1). *A*, I–V plot for an RB cell from a 5-d-old larva. The current reversed at −40 mV. *B*, I–V plot for a DLi cell from a 4-d-old larva. The current reversed at −57 mV. *C*, Histogram of perforated patch GABA E_{Rev} for RB cells (*open bars*) and DLi cells (*solid bars*); mean values are *inset*. All data were recorded using amphotericin B and solutions B8 and PP1 or PP2; 3- to 8-d-old larvae.

Table 2. GABA reversal potentials in perforated patch recordings

	Condition	E_{Rev}
RB cells:	1. Normal saline ($+Na^+$)	−38 ± 3 mV (22)
	2. 0-Na^+/0-Na^+, 0-K^+	−48 ± 11 mV (9)[a,b]
	3. + Bumetanide	−47 ± 4 mV (9)[a,b]
DLi cells:	4. Normal saline	−63 ± 7 mV (31)[a]
	5. 0-Na^+	−68 ± 6 mV (11)[a,c]
	6. + Bumetanide	−61 ± 8 mV (12)[a,c]
	7. + Bumetanide, + Ethacrynic acid	−65 ± 15 mV (5)[a,c]

Values for DLi cells in normal external saline using either amphotericin B or gramicidin did not differ (see text) and are pooled in line 4.

[a] Significantly different from RB cell E_{Rev} in normal saline.

[b] Significantly different from DLi cell E_{Rev} in normal saline.

[c] Not significantly different from DLi cell E_{Rev} in normal saline.

vide an estimate of $[Cl^-]_i$ when a direct measurement, such as with ion-selective microelectrodes (Alvarez-Leefmans et al., 1988), is not feasible. This approach assumes that $[Cl^-]_i$ does not change significantly with time because of equilibration of Cl^- through the perforated patch. Nystatin and amphotericin B, two commonly used pore-forming antibiotics, have significant Cl^- permeability, although the permeability is less than one-tenth that of monovalent cations (Cass et al., 1970; Marty and Finkelstein, 1975; Russell et al., 1977; Kleinberg and Finkelstein, 1984). Depending on $[Cl^-]$ in the recording pipette and the length of the recording, a considerable change in $[Cl^-]_i$ may occur over time when nystatin is used; this problem is alleviated by the use of gramacidin as the perforant (Rhee et al., 1994; Kyrozis and Reichling, 1995). However, our observation that DLi cell E_{Rev} did not differ between amphotericin B and gramicidin recordings indicates that $[Cl^-]_i$ was not altered significantly by equilibration between pipette and cell. In the larger RB cells, it is unlikely that Cl^- equilibration affected the estimation of $[Cl^-]_i$, although technical difficulties precluded directly verifying this with gramicidin recordings. Under the present conditions, the perforated patch E_{Rev} of −38 mV for RB cells vs −63 mV for DLi cells is consistent with a two- to threefold higher $a[Cl^-]_i$ in RB cells.

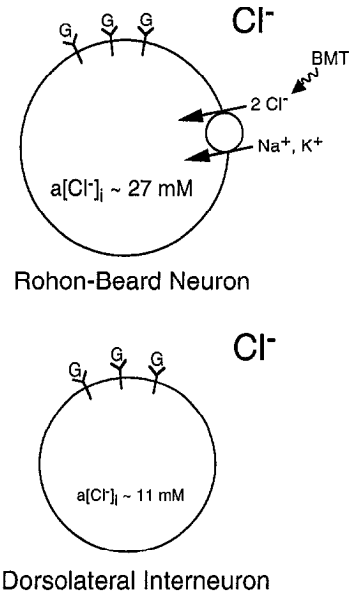

Figure 7. Model for the regulation of $[Cl^-]_i$ in RB and DLi cells. RB neuron and dorsolateral interneuron with $GABA_A$ receptors are schematized. A Na^+-dependent, bumetanide-sensitive Cl^- cotransporter is represented in the RB membrane. Internal Cl^- activities are estimated from the mean perforated patch E_{Rev} for each cell type. In RB cells, inwardly directed Cl^- transport contributes to an $a[Cl^-]_i$ that is more than twofold greater than that of DLi cells. *G*, GABA; *BMT*, bumetanide.

We have considered so far, as is widely assumed, that E_{GABA} is equivalent to E_{Cl}. Alternatively, E_{Rev} for $GABA_A$ and glycine receptor responses could be influenced by other permeant anions such as bicarbonate, which has a relative permeability of ~0.2 compared with Cl^- in mammalian $GABA_A$ receptors (Bormann et al., 1987). HCO_3^- contributes significantly to the depolarizing GABA IPSP in neocortical neurons, where the intracellular concentration was estimated to be 10–20 mM (Kaila et al., 1993). Because we have used salines buffered with HEPES and without CO_2 equilibration, $a[HCO_3^-]_i$ is likely to be negligible. However, calculations show that even for an $a[HCO_3^-]_i$ of 10–20 mM, $a[Cl^-]_i$ must be twofold higher in RB cells than in DLi cells to account for the difference in E_{Rev}.

Removal of external Na^+ and exposure to bumetanide produce similar negative shifts in RB cell E_{Rev}, but less than half as large as the observed 25 mV difference between RB and DLi cells in standard saline. The shift in Na^+-free saline is larger in intracellular recordings from RB cells, possibly because the exposure time in perforated patch recordings was insufficiently long or because the transport mechanism was compromised by the recording technique. Although we found no evidence for Na^+-dependent Cl^- transport in DLi cells, it is possible that outward transport was not detected under conditions in which $[Cl^-]_i$ was normally low. In mammalian neurons that maintain a low $[Cl^-]_i$, evidence for furosemide-sensitive outward Cl^- transport has been demonstrated after elevation of $[Cl^-]_i$ by injection or chronic membrane depolarization (Misgeld et al., 1986; Thompson et al., 1988). The difference in the GABA E_{Rev} of intact RB and DLi cells also could be influenced by other factors, including different passive distributions of Cl^- or an unusually elevated $[HCO_3^-]_i$ in RB cells.

Our results indicate that both depolarizing and hyperpolarizing $GABA_A$ receptor-mediated responses are present at the same time in two neighboring populations of embryonic spinal neurons, in contrast with recent studies in the mammalian CNS, which emphasize the transition in GABA responses from predominantly depolarizing to hyperpolarizing over the first few weeks of life. Spontaneous and evoked synaptic potentials mediated by $GABA_A$ receptors are depolarizing (Mueller et al., 1984; Ben-Ari et al., 1989; Cherubini et al., 1990; Luhmann and Prince, 1991), and exogenous application of $GABA_A$ agonists similarly generates depolarizations in embryonic hippocampal (Mueller et al., 1984; Janigro and Schwartzkroin, 1988b), cortical (Luhmann and Prince, 1991), and spinal neurons (Mandler et al., 1990; Wu et al., 1992). Inwardly directed Cl^- transport has been proposed to account for these results, but there has been no direct evidence previously from embryonic or immature neurons to support this hypothesis.

Depolarizing $GABA_A$ responses are found in the adult CNS as well, including amphibian and mammalian dorsal root neurons (Nicoll, 1978; Wojtowicz and Nicoll, 1982; Gallagher et al., 1983) and mammalian hippocampal neurons (Andersen et al., 1980; Misgeld et al., 1986; Janigro and Schwartzkroin, 1988a; Lambert et al., 1991; Michelson and Wong, 1991; Grover et al., 1993). The involvement of Cl^- transporters has been difficult to resolve in part because Cl^- transport inhibitors were found in some cases to

directly depress the Cl^- conductance, rather than having the expected effect of shifting the GABA E_{Rev} (Nicoll, 1978; Gallagher et al., 1983). In hippocampal neurons, spatial differences in $[Cl^-]_i$ have been indicated by depolarizing and hyperpolarizing responses when GABA is applied to dendritic and somatic regions, respectively. Such spatial differences in Cl^- gradients may be regulated by both inwardly and outwardly directed furosemide-sensitive Cl^- transporters or pumps in different regions of the same cell (Misgeld et al., 1986; Müller et al., 1989). Recent work resolves these issues with a model in which high-frequency $GABA_A$ receptor activation leads to shifts in Cl^- and HCO_3^- gradients that support depolarization in distal dendrites (Staley et al., 1995).

By 30 hr of age, nearly 100% of RB cells *in vivo* respond to GABA with depolarization; in addition, ~40% respond similarly to glycine (Bixby and Spitzer, 1982). Although a source of neurotransmitter input to RB cells is not presently known, their longitudinal processes run in the same tract with GABAergic interneurons (Roberts and Clarke, 1982; Roberts et al., 1987) and may be contacted by them. At the time that RB cells become sensitive to these transmitters, the action potential is prolonged with inward current carried mainly by Ca^{2+} ions (Baccaglini and Spitzer, 1977). Spontaneously generated, transient elevations of $[Ca^{2+}]_i$ in cultured *Xenopus* spinal neurons during this early, Ca^{2+}-sensitive period are important for several aspects of neuronal differentiation, including neurite extension, acquisition of GABA immunoreactivity, and accelerated potassium current activation (Holliday and Spitzer, 1990; Desarmenien and Spitzer, 1991; Spitzer et al., 1993; Gu and Spitzer, 1995). GABA and glycine evoke depolarizations and elevate $[Ca^{2+}]_i$ in developing mammalian spinal neurons (Wu et al., 1992; Reichling et al., 1994; Wang et al., 1994) and in cortical and cerebellar neurons (Connor et al., 1987; Yuste and Katz, 1991). Thus, the potential for these transmitters to stimulate Ca^{2+} elevations in RB cells via Cl^--mediated depolarization prompts further investigation of their role in the developing spinal cord.

REFERENCES

Alvarez-Leefmans FJ, Gamiño SM, Giraldez F, Noguerón I (1988) Intracellular chloride regulation in amphibian dorsal root ganglion neurons studied with ion-selective microelectrodes. J Physiol (Lond) 406:225–246.

Andersen P, Dingledine R, Gjerstad L, Langmoen IA, Laursen AM (1980) Two different responses of hippocampal pyramidal cells to application of gamma-aminobutyric acid. J Physiol (Lond) 305:279–296.

Baccaglini PI, Spitzer NC (1977) Developmental changes in the inward current of the action potential of Rohon-Beard neurones. J Physiol (Lond) 271:93–117.

Ben-Ari Y, Cherubini E, Corradetti R, Gaiarsa JL (1989) Giant synaptic potentials in immature rat CA3 hippocampal neurones. J Physiol (Lond) 416:303–325.

Bixby JL, Spitzer NC (1982) The appearance and development of chemosensitivity in Rohon-Beard neurones of the *Xenopus* spinal cord. J Physiol (Lond) 330:513–536.

Bormann J, Hamill OP, Sakmann B (1987) Mechanism of anion permeation through channels gated by glycine and gamma-aminobutyric acid in mouse cultured spinal neurones. J Physiol (Lond) 385:243–286.

Cass A, Finkelstein A, Krespi V (1970) The ion permeability induced in thin lipid membranes by the polyene antibiotics nystatin and amphotericin B. J Gen Physiol 56:100–124.

Cherubini E, Gaiarsa JL, Ben-Ari Y (1991) GABA: an excitatory transmitter in early postnatal life. Trends Neurosci 14:515–519.

Cherubini E, Rovira C, Gaiarsa JL, Corradetti R, Ben-Ari Y (1990) GABA mediated excitation in immature rat CA3 hippocampal regions. Int J Dev Neurosci 8:481–490.

Clarke JDW, Roberts A (1984) Interneurones in the *Xenopus* embryo spinal cord: sensory excitation and activity during swimming. J Physiol (Lond) 354:345–362.

Connor JA, Tseng H-Y, Hockberger PE (1987) Depolarization- and transmitter-induced changes in intracellular Ca^{2+} of rat cerebellar granule cells in explant cultures. J Neurosci 7:1384–1400.

Desarmenien MG, Spitzer NC (1991) Determinant role of calcium and protein kinase C in development of the delayed rectifier potassium current in *Xenopus* spinal neurons. Neuron 7:797–805.

Gallagher JP, Nakamura J, Shinnick-Gallagher P (1983) The effects of temperature, pH and Cl-pump inhibitors on GABA responses recorded from cat dorsal root ganglia. Brain Res 267:249–259.

Grover LM, Lambert NA, Schwartzkroin PA, Teyler TJ (1993) Role of HCO_3^- ions in depolarizing $GABA_A$ receptor-mediated responses in pyramidal cells of rat hippocampus. J Neurophysiol 69:1541–1554.

Gu X, Spitzer NC (1995) Distinct aspects of neuronal differentiation encoded by frequency of spontaneous Ca^{2+} transients. Nature 375: 784–787.

Haas M (1989) Properties and diversity of (Na-K-Cl) cotransporters. Annu Rev Physiol 51:443–457.

Hara M, Inoue M, Yasukura T, Ohnishi S, Mikami Y, Inagaki C (1992) Uneven distribution of intracellular Cl^- in rat hippocampal neurons. Neurosci Lett 143:135–138.

Hladky SB, Haydon DA (1984) Ion movements in gramicidin channels. Curr Top Membr Transp 21:327–372.

Holliday J, Spitzer NC (1990) Spontaneous calcium influx and its roles in differentiation of spinal neurons in culture. Dev Biol 141:13–23.

Horn R, Marty A (1988) Muscarinic activation of ionic currents measured by a new whole-cell recording method. J Gen Physiol 92:145–159.

Janigro D, Schwartzkroin PA (1988a) Effects of GABA on CA3 pyramidal cell dendrites in rabbit hippocampus. Brain Res 453:265–274.

Janigro D, Schwartzkroin PA (1988b) Effects of GABA and baclofen on pyramidal cells in the developing rabbit hippocampus. Brain Res 469:171–184.

Kaila K, Voipio J, Paalasmaa P, Pasternack M, Deisz RA (1993) The role of bicarbonate in $GABA_A$ receptor-mediated IPSPs of rat neocortical neurons. J Physiol (Lond) 464:273–289.

Kleinberg ME, Finkelstein A (1984) Single-length and double-length channels formed by nystatin in lipid bilayer membranes. J Membr Biol 80:257–269.

Kyrozis A, Reichling DB (1995) Perforated-patch recording with gramicidin avoids artifactual changes in intracellular chloride concentration. J Neurosci Methods 57:27–35.

Lambert NA, Borroni AM, Grover LM, Tehler TJ (1991) Hyperpolarizing and depolarizing $GABA_A$ receptor-mediated dendritic inhibition in area CA1 of the rat hippocampus. J Neurophysiol 66:1538–1548.

Luhmann HJ, Prince DA (1991) Postnatal maturation of the GABAergic system in rat neocortex. J Neurophysiol 65:247–263.

MacDonald RL, Olsen RW (1994) $GABA_A$ receptor channels. Annu Rev Neurosci 17:569–602.

Mandler RN, Scahner AE, Novotny EA, Lange GD, Smith SV, Barker JL (1990) Electrical and chemical excitability appear one week before birth in the embryonic rat spinal cord. Brain Res 522:46–54.

Marty A, Finkelstein A (1975) Pores formed in lipid bilayer membrane by nystatin: differences in its one-sided and two-sided action. J Gen Physiol 65:515–526.

Michelson HB, Wong RKS (1991) Excitatory synaptic responses mediated by $GABA_A$ receptors in the hippocampus. Science 253:1420–1423.

Misgeld U, Deisz RA, Dodt HU, Lux HD (1986) The role of chloride transport in postsynaptic inhibition of hippocampal neurons. Science 232:1413–1415.

Mueller AL, Taube JS, Schwartzkroin PA (1984) Development of hyperpolarizing inhibitory postsynaptic potentials and hyperpolarizing responses to γ-aminobutyric acid in rabbit hippocampus studied *in vitro*. J Neurosci 4:860–867.

Müller W, Misgeld U, Lux HD (1989) γ-Aminobutyric acid-induced ion movements in the guinea pig hippocampal slice. Brain Res 484: 184–191.

Neher E (1992) Correction for liquid junction potentials in patch clamp experiments. Methods Enzymol 207:123–131.

Nicoll RA (1978) The blockade of GABA mediated responses in the frog spinal cord by ammonium ions and furosemide. J Physiol (Lond) 283:121–132.

Nieuwkoop PD, Faber J (1965) Normal tables for *Xenopus laevis*, 2nd Ed (Daudin). Amsterdam: North-Holland.

Rae J, Cooper K, Gates G, Watsky M (1991) Low access resistance perforated patch recordings using amphotericin B. J Neurosci Methods 37:15–26.

Reichling DB, Kyrozis A, Wang J, MacDermott AB (1994) Mechanisms of GABA and glycine depolarization-induced calcium transients in rat dorsal horn neurons. J Physiol (Lond) 476:411–421.

Rhee J-S, Ebihara S, Akaike N (1994) Gramicidin perforated patch-clamp technique reveals glycine-gated outward chloride current in dissociated nucleus solitarii neurons of rat. J Neurophysiol 72:1103–1108.

Roberts A, Clarke JDW (1982) The neuroanatomy of an amphibian embryo spinal cord. Philos Trans R Soc Lond [Biol] 296:195–212.

Roberts A, Dale N, Otterson OP, Storm-Mathisen J (1987) The early development of neurons with GABA immunoreactivity in the CNS of *Xenopus laevis* embryos. J Comp Neurol 261:435–449.

Robinson RA, Stokes RH (1965) Electrolyte solutions: the measurement and interpretation of conductance, chemical potential and diffusion in solutions of simple electrolytes, 2nd Ed. London: Butterworths.

Rohrbough J, Spitzer NC (1994) Depolarizing and hyperpolarizing GABA responses in *Xenopus* spinal neurons are mediated by $GABA_A$ receptors. Soc Neurosci Abstr 20:1725.

Russell JM, Eaton DC, Brodwick MS (1977) Effects of nystatin on membrane conductance and internal ion activities in *Aplysia* neurons. J Membr Biol 37:137–156.

Sillar KT, Roberts A (1991) Segregation of NMDA and non-NMDA receptors at separate synaptic contacts: evidence from spontaneous EPSPs in *Xenopus* embryo spinal neurones. Brain Res 545:24–32.

Sillar KT, Simmers J (1994) Presynaptic inhibition of primary afferent transmitter release by 5-hydroxytryptamine at a mechanosensory synapse in the vertebrate spinal cord. J Neurosci 14:2636–2647.

Spitzer NC, deBaca RC, Allen KA, Holliday J (1993) Calcium dependence of differentiation of GABA immunoreactivity in spinal neurons. J Comp Neurol 337:168–175.

Staley KJ, Soldo BL, Proctor WR (1995) Ionic mechanisms of neuronal excitation by inhibitory $GABA_A$ receptors. Science 269:977–981.

Thompson SM, Deisz RA, Prince DA (1988) Relative contributions of passive equilibrium and active transport to the distribution of chloride in mammalian cortical neurons. J Neurophysiol 60:105–124.

Wang J, Reichling DB, Kyrozis A, MacDermott AB (1994) Developmental loss of GABA- and glycine-induced depolarization and Ca^{2+} transients in embryonic rat dorsal horn neurons in culture. J Neurosci 6:1275–1280.

Wojtowicz JM, Nicoll RA (1982) Selective action of piretanide on primary afferent GABA responses in the frog spinal cord. Brain Res 236:173–181.

Wu W-l, Ziskind-Conhaim L, Sweet MA (1992) Early development of glycine- and GABA-mediated synapses in rat spinal cord. J Neurosci 12:3935–3945.

Yuste R, Katz LC (1991) Control of postsynaptic Ca^{2+} influx in developing neocortex by excitatory and inhibitory neurotransmitters. Neuron 6:333–344.

Zhang L, Spigelman I, Carlen PL (1991) Development of GABA-mediated, chloride-dependent inhibition in CA1 pyramidal neurones of immature rat hippocampal slices. J Physiol (Lond) 444:25–49.